Journal of Catalysis **186,** 181–187 (1999)
Article ID jcat.1999.2535, available online at http://www.idealibrary.com on IDEAL®

Partial Oxidation of Methane to Synthesis Gas over MgO- and SiO_2-Supported Rhodium Catalysts

H. Y. Wang and E. Ruckenstein[1]

Department of Chemical Engineering, State University of New York at Buffalo, Amherst, New York 14260

Received January 28, 1999; revised April 19, 1999; accepted April 20, 1999

The partial oxidation of methane over MgO- and SiO_2-supported rhodium catalysts was investigated, using a CH_4/O_2 mixture with a molar ratio of 2.1/1 as feed gas. At 750°C and atmospheric pressure, the 1% Rh/MgO catalyst exhibited a very high stability at the high gas hourly space velocity of 720,000 ml g^{-1} h^{-1}, its catalytic activity and selectivity remaining constant and high after an induction time up to 100 h of reaction. In contrast, the 1% Rh/SiO_2 catalyst deactivated rapidly. To explain the above results, the reaction behaviors of CH_4 and CH_4/O_2 (2/1) over the oxidized catalysts 1% Rh(O)/MgO and 1% Rh(O)/SiO_2 were studied in a pulse microreactor. No carbon deposition occurred during the reaction of CH_4 with the MgO-supported rhodium catalyst, even after the catalyst was almost completely reduced. In contrast, a notable amount of surface carbon was generated during the reaction of CH_4 with the SiO_2-supported rhodium catalyst. During the reaction of CH_4/O_2 (2/1) over the oxidized catalysts, the rhodium oxide supported on SiO_2 was easily reduced by CH_4, while the reduction of rhodium oxide supported on MgO occurred with some difficulty. This implies much stronger interactions between rhodium oxide and MgO than between the former and SiO_2. Temperature-programmed reduction experiments also revealed much stronger interactions between rhodium and magnesium oxide and that two kinds of rhodium compounds were present in the oxidized MgO-supported rhodium catalyst. X-ray powder diffraction enabled us to identify Rh_2O_3 and $MgRh_2O_4$ in precalcined 10% Rh(O)/SiO_2 and 10% Rh(O)/MgO, respectively. It is suggested that the strong interactions between rhodium and magnesium oxide (especially the formation of $MgRh_2O_4$) are responsible for the high stability of the MgO-supported rhodium catalysts.

Key Words: **methane partial oxidation; syngas; rhodium supported on magnesia; rhodium supported on silica; magnesium rhodium oxide.**

1. INTRODUCTION

The chemical utilization of natural gas, one of the world's abundant resources, to produce basic chemicals is one of the desirable goals of the current chemical industry. The conversion of methane to useful chemicals has attracted attention in recent years and many technologies have been developed. Although the direct conversion of methane to valuable chemicals such as ethylene (1, 2) or methanol and formaldehyde (3) is a most fascinating route, no viable process or catalyst has yet been developed. For the time being, indirect transformation of methane via synthesis gas is still the most competitive process (4). Partial oxidation is a promising approach for producing synthesis gas from methane and oxygen or air (reaction 1). The reaction is mildly exothermic and produces a syngas with a H_2/CO ratio of about 2, a composition suitable for methanol, and Fischer–Tropsch syntheses (5, 6). This process is more energy efficient and can produce a H_2/CO ratio more suitable than that provided by steam reforming (reaction 2) or by CO_2 reforming (reaction 3).

$$CH_4 + 1/2\,O_2 \rightarrow CO + 2\,H_2 \qquad \Delta H^0_{298} = -36\ \text{kJ/mol} \quad [1]$$

$$CH_4 + H_2O \rightarrow CO + 3\,H_2 \qquad \Delta H^0_{298} = 206\ \text{kJ/mol} \quad [2]$$

$$CH_4 + CO_2 \rightarrow 2\,CO + 2\,H_2 \qquad \Delta H^0_{298} = 247\ \text{kJ/mol} \quad [3]$$

The catalysts used for this reaction are mainly supported noble metals, such as Rh, Ru, Pd, and Pt (7–14), and supported Ni catalysts (15–26), as well as some pyrochlore type oxides ($Ln_2Ru_2O_7$) (27, 28) and perovskite type oxides ($LaMO_3$; M = Ni, Rh, Co, Cr) (29–31).

The selection of a heterogeneous catalyst for a given reaction should be based on a high conversion of reactants to desired products, but also on the stability of the catalyst, which should maintain high activity and selectivities for a sufficiently long time under the particular conditions of operation. In the methane partial oxidation reaction, the sintering and the deposition of carbonaceous materials are two common factors leading to the deactivation of the catalyst. It has been demonstrated that the rate of coke formation during the steam reforming of hydrocarbons depends on the metal crystallite size over supported nickel catalysts (32). The aggregation of metal caused by sintering accelerates the rate of coke formation. The most obvious way to lessen sintering is to keep the temperature low. Unfortunately, the methane partial oxidation reaction has to proceed at high temperatures (usually >700°C) to get a meaningful conversion of methane.

[1] To whom correspondence should be addressed.

0021-9517/99 $30.00

The tendency for coke deposition is considered to be the main drawback of supported nickel catalysts, because it leads to their rapid deactivation. Many studies have been conducted to develop coke-resistant nickel catalysts. It has been proposed that the formation of a NiO/MgO solid solution in the catalyst precursor is responsible for the stability observed over MgO-supported nickel catalysts (24, 33, 34). For catalysts containing noble metals, Slagtern and Olsbye reported that $LaRhO_3$ can provide a 95% methane conversion and 98% CO selectivity even after 120 h of reaction at 800°C (29). However, the content of rhodium in their catalyst was high (around 35 wt%) and the residence time was also high (1 s). Generally one considers that Rh provides a high and stable syngas yield in the partial oxidation of methane, more stable than other metals. It will be shown here that the support affects its behavior by comparing the Rh/MgO- and Rh/SiO_2-supported catalysts. In this paper, the magnesium oxide supported rhodium catalyst with 1% Rh content is reported to have high activity and selectivity as well as high stability under the extremely high gas hourly space velocity (GHSV) of 720,000 ml g^{-1} h^{-1}. In contrast, the 1% Rh/SiO_2 has a low stability. Pulse reactions, temperature-programmed reduction (TPR), and X-ray powder diffraction (XRD) were used to characterize the catalysts to explain their behavior. Much stronger interactions between rhodium and support were detected for the Rh/MgO catalyst than for the Rh/SiO_2 catalyst. The strong interactions between rhodium and magnesium oxide are most likely responsible for the high stability of the Rh/MgO catalyst.

2. EXPERIMENTAL

2.1. Catalyst Preparation

The MgO (or SiO_2)-supported rhodium catalysts were prepared by impregnating MgO (or SiO_2) with a $Rh(NO_3)_3 \cdot 2H_2O$ ethanol solution, followed by overnight drying at 110°C and calcination in air at 800°C for 4 h. The calcined catalysts are denoted as Rh(O)/MgO (or SiO_2). The catalysts reduced in H_2 are denoted as Rh/MgO (or SiO_2). Rh loading means the wt% Rh in the reduced catalyst.

2.2. Catalytic Reaction

2.2.1. Activity assay. All activity assays were conducted under atmospheric pressure in a fixed-bed flow vertical quartz reactor (3 mm inside diameter) located in an electronically controlled furnace, with the catalyst powder held on quartz wool. Five milligrams of catalyst (about 2.5 mm height) was used in each run. The prepared catalyst was heated in a H_2 flow (20 ml/min) up to 750°C, after which H_2 was switched to a CH_4/O_2 mixture with a molar ratio of 2.1 to carry out the reaction at a GHSV of 720,000 ml g^{-1} h^{-1} and a furnace temperature of 750°C. The reactants and products were analyzed with an on-line gas chromatograph equipped with Porapak Q and 5A molecular sieve columns. A thermocouple was inserted in the middle of the catalyst bed to measure the temperature of the catalyst and another was located in the gas near the exit of the catalyst bed to measure the temperature of the gaseous phase.

2.2.2. Pulse reaction. A quartz tube (4 mm inside diameter) was used as reactor with the catalyst held on quartz wool. During the pulse experiments, there was a constant flow of helium (35 ml/min) through the reactor, and the reactant gas mixture was injected in the carrier gas. In each run, 50.0 mg of catalyst was used. The pulse volume was 50 μl for both CH_4 and CH_4/O_2 (2/1). The reactants and products were analyzed with an on-line gas chromatograph equipped with a thermal conductivity detector (TCD) and a Porapak Q column.

2.3. Catalyst Characterization

2.3.1. Surface area. The surface areas of the calcined catalysts were determined via nitrogen adsorption, using a Micromeritrics ASAP2000 instrument. The sample was degassed at 200°C for at least 5 h in high vacuum before the measurement. The surface areas were 42.8 m^2/g for 1% Rh(O)/MgO and 573.7 m^2/g for 1% $Rh(O)/SiO_2$.

2.3.2. Dispersion of the metal. The Rh dispersion of the reduced catalysts was determined by CO chemisorption at room temperature and the stoichiometry of CO to metallic Rh was assumed to be 1/1. One hundred milligrams of calcined catalyst powder held on quartz wool was reduced in a H_2 flow (20 ml/min) at 500°C for 1.5 h. Further, at the same temperature, the reduced catalyst was purged with an ultra high purity helium flow (35 ml/min) for 1 h. After the temperature was decreased to room temperature, CO (10 μl per pulse) was pulsed over the catalyst until no further adsorption of CO was detected. The CO left in CO chemisorption was determined quantitatively with a TCD. Both the hydrogen and helium were further purified with a Hydro-Purge II and an Oxy-Trap column before use. The initial dispersions of Rh after reduction were 3.9% for 1% Rh/MgO and 9.0% for 1% Rh/SiO_2.

2.3.3. Temperature-programmed reduction. TPR of the calcined catalyst was conducted by heating the sample from 50 to 950°C at a rate of 20°C/min in a flow of 2.5% H_2/Ar mixture (35 ml/min). The hydrogen consumed in TPR was determined with a TCD. Twenty-five milligrams of sample precalcined in air at 800°C for 4 h was used in each TPR run.

2.3.4. X-ray powder diffraction. XRD was carried out with a Siemens D500 X-ray diffractometer, using Cu $K\alpha$ radiation, at 40 kV and 30 mA.

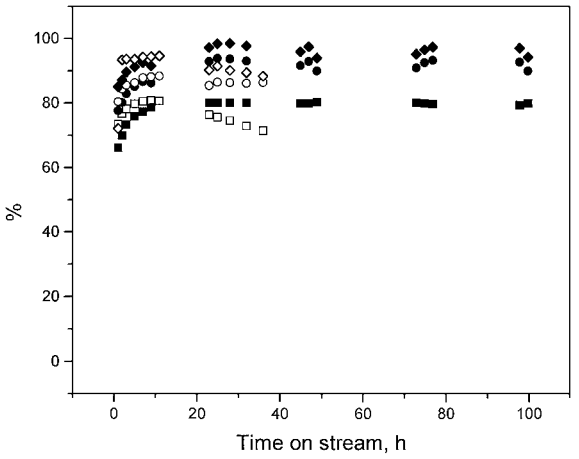

FIG. 1. CH_4 conversion (square), CO selectivity (circle), and H_2 selectivity (diamond) obtained over the reduced 1% Rh/MgO (solid) and 1% Rh/SiO_2 (open) catalysts in the continuous reaction. $P = 1$ atm, $T_{\text{furnace}} = 750°C$, $CH_4/O_2 = 2.1$, GHSV = 720,000 ml g^{-1} h^{-1}.

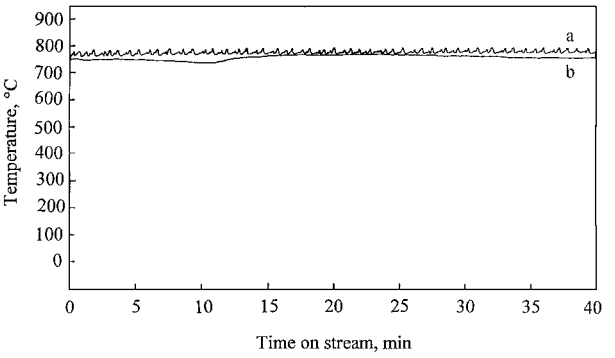

FIG. 2. Relationship between catalyst temperature and reaction time over 1% Rh/SiO_2 (a) and 1% Rh/MgO (b) in the continuous reaction.

3. RESULTS

3.1. Continuous Flow Reaction

3.1.1. Effect of time on stream. A CH_4/O_2 gas mixture with a molar ratio of 2.1/1 was used as feed gas and the partial oxidation reaction was conducted under atmospheric pressure at 750°C (furnace temperature) and at a GHSV of 720,000 h^{-1} over MgO- and SiO_2-supported rhodium catalysts. The effect of time on stream was investigated and the results are presented in Fig. 1. During the first 10 h of reaction, the methane conversion over 1% Rh/SiO_2 was higher than that over 1% Rh/MgO. However, after 20 h of reaction, both the methane conversion and the selectivities to CO and H_2 over 1% Rh/MgO became higher than those over 1% Rh/SiO_2. In addition, while the activity over 1% Rh/SiO_2 decayed rapidly after 20 h, the activity and the selectivities to CO and H_2 over 1% Rh/MgO remained unchanged up to at least 100 h of reaction. The 1% Rh/MgO catalyst provides about 80% methane conversion, 92% CO selectivity, and 96% H_2 selectivity, with very high stability.

The temperature of the catalyst was recorded during the reaction. The temperature profile recorded during the first 40 min of reaction is shown in Fig. 2. The catalyst temperature for 1% Rh/SiO_2 oscillated with an amplitude of about 25°C around an average temperature of about 770°C, while no such oscillations were observed for the 1% Rh/MgO catalyst. A similar observation was reported previously (35) for SiO_2- and MgO-supported nickel catalysts.

3.2. Pulse Reaction

3.2.1. Interaction of CH_4 pulses with the 1% Rh(O)/MgO and 1% Rh(O)/SiO_2 catalysts. The interactions of methane pulses with the 1% Rh(O)/MgO- and 1% Rh(O)/SiO_2-supported Rh catalysts were investigated at 750°C. The amount of surface carbon formed was evaluated from the carbon balance. Figure 3 presents the variations of methane conversion and selectivities to CO, CO_2, and C (surface carbon) over the 1% Rh(O)/MgO catalyst as a function of the number of CH_4 pulses. Based on carbon

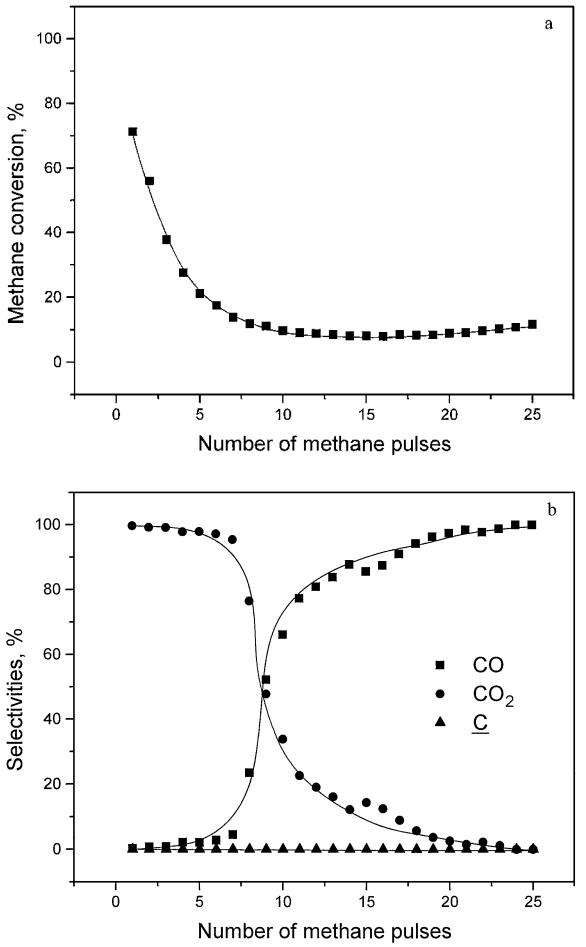

FIG. 3. The relationship of methane conversion (a) and selectivities to CO, CO_2, and C (b) with the number of methane pulses over 1% Rh(O)/MgO at 750°C.

balance, one can conclude that no surface carbon was formed during the reaction of CH_4 with the 1% Rh(O)/MgO catalyst. With the increase in the number of CH_4 pulses, the methane conversion decreased sharply during the first 7 pulses, decreased gradually during the following 9 pulses, and slightly increased after the 16th pulse. During the first 7 pulses, only a small amount of CO (<5%) was formed and no H_2 was detected, the reaction being dominated by the formation of CO_2 and H_2O. Since no O_2 was present in the feed gas, it is clear that the oxygen of the catalyst was responsible for the formation of CO_2 and H_2O. With the rapid depletion of the active oxygen of the catalyst during the first several pulses, the methane conversion decreased sharply as observed in Fig. 3a. Starting with the 8th pulse, H_2 was detected as one of the products and the selectivity to CO increased sharply to about 77% at the 11th pulse, after which it increased more gradually until it reached 100% at the 24th pulse (Fig. 3b). From the 10th pulse onward, the formation of CO and H_2 dominated the reaction even though the corresponding methane conversion was low (around 10%).

For comparison purposes, the interaction of CH_4 with the oxidized 1% Rh(O)/SiO_2 was also investigated and the results are plotted in Fig. 4. During the first 6 pulses, the methane conversion was high (≥90%). Starting with the 7th pulse, the methane conversion decreased rapidly for the following 5 pulses and gradually from the 13th to the 25th pulse (Fig. 4a). Unlike the 1% Rh(O)/MgO, surface carbon was formed over the 1% Rh(O)/SiO_2 during each pulse. During the first pulse, no CO or H_2 was detected, and the CO_2 formation dominated. At the 2nd pulse, both H_2 and CO were detected, and the amount of CO_2 decreased to a very low level (<0.5%). Starting with the 2nd pulse, the surface carbon formation dominated the reaction (Fig. 4b). It is clear that the SiO_2-supported rhodium catalyst has a high capacity for methane conversion and decomposition and that the carbon deposition is mainly responsible for the deactivation observed in Fig. 4a.

3.2.2. Reaction of CH_4/O_2 pulses over the 1% Rh(O)/MgO and 1% Rh(O)/SiO_2 catalysts. The reactions of methane and oxygen over the oxidized catalysts were investigated by generating pulses of CH_4/O_2 mixture with a stoichiometric feed ratio of 2/1. O_2 was completely consumed during each pulse reaction. The product formed contained CO, H_2, CO_2, and H_2O. The carbon balance indicated that no carbon was deposited on the catalyst. In Figs. 5a and 5b, the reactivities of CH_4/O_2 over 1% Rh(O)/MgO and over 1% Rh(O)/SiO_2 are compared at 750°C; major differences can be observed. For the 1st pulse, methane was converted completely over both catalysts and no CO or H_2 was formed, CO_2 being the only carbon-containing product generated. Starting with the 2nd pulse, the methane conversion remained at 100% over 1% Rh(O)/SiO_2, while over 1% Rh(O)/MgO it decreased sharply, becoming 45.5% at the 5th pulse, and then increased gradually to 73.2% at the 15th pulse. Over 1% Rh(O)/SiO_2, CO and H_2 were formed starting with the 2nd pulse and the CO selectivity increased sharply to 96.0% at the third pulse, remaining around 97% from the 5th pulse onward. Over 1% Rh(O)/MgO, CO started to form at the 4th pulse, but H_2 was not formed until the 6th pulse. With the increase in the number of pulses, the CO selectivity increased rapidly from 2.0% at the 4th pulse to 81.6% at the 7th pulse and then it increased gradually to 93.4% at the 15th pulse.

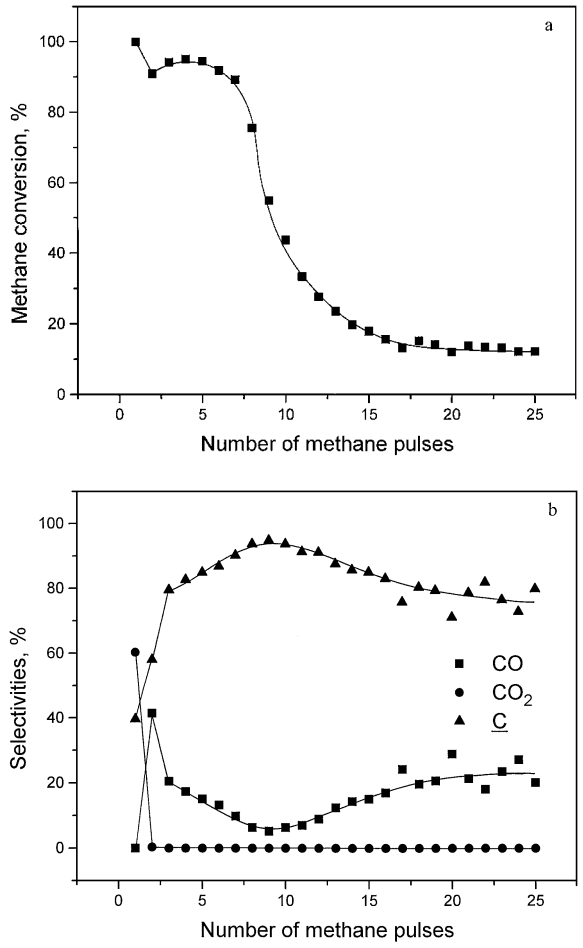

FIG. 4. The relationship of methane conversion (a) and selectivities to CO, CO_2, and C (b) with the number of methane pulses over 1% Rh(O)/SiO_2 at 750°C.

3.3. The Reductivities of the 1% Rh(O)/MgO and 1% Rh(O)/SiO_2 Catalysts

The reductivities of the 1% Rh(O)/MgO and 1% Rh(O)/SiO_2 catalysts were investigated by means of TPR. As shown in Fig. 6, 1% Rh(O)/SiO_2 exhibits only one peak at about 140°C with a long tail and 1% Rh(O)/MgO exhibits two peaks at about 350 and 530°C.

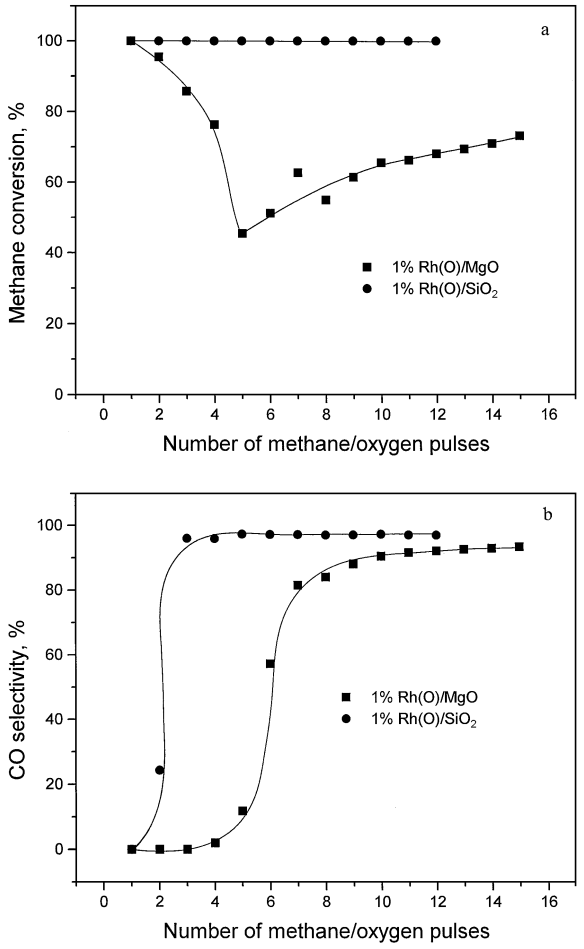

FIG. 5. Comparison of methane conversion (a) and CO selectivity (b) during CH_4/O_2 (2/1) reaction over 1% Rh(O)/MgO and 1% Rh(O)/SiO_2 at 750°C.

3.4. XRD Results

Because the rhodium content of 1% Rh(O)/MgO and 1% Rh(O)/SiO_2 was too low for XRD analysis, 10% Rh(O)/support samples were prepared to obtain information about the rhodium compound(s) present in the catalysts. The XRD patterns of 10% Rh(O)/SiO_2 provided peaks at $2\theta = 23.8, 32.8, 34.9, 48.6, 53.2, 61.2$, and 62.6, which can be attributed to Rh_2O_3. For the 10% Rh(O)/MgO, besides the peaks at $2\theta = 42.4$ and 61.6 belonging to MgO, additional peaks at $2\theta = 18.0$, 34.8, 36.4, and 56.0 were present, which can be attributed to $MgRh_2O_4$. In conclusion, Rh_2O_3 and $MgRh_2O_4$ were detected over 10% Rh(O)/SiO_2 and 10% Rh(O)/MgO, respectively. $MgRh_2O_4$ (magnesium rhodium oxide) has a spinel structure.

4. DISCUSSION

The low-temperature reduction peak around 140°C in the TPR curve of the 1% Rh(O)/SiO_2 catalyst (Fig. 6) indicates a facile reduction of rhodium oxide supported on SiO_2, implying that there are weak interactions between rhodium and SiO_2. In contrast, the two peaks at much higher temperatures, 350 and 530°C, in the TPR curve of the 1% Rh(O)/MgO catalyst (Fig. 6) imply that there are much stronger interactions between rhodium and magnesium oxide and that two kinds of rhodium compounds are present in the 1% Rh(O)/MgO catalyst. According to the XRD results, $MgRh_2O_4$ was present in the precalcined 10% Rh(O)/MgO sample. Since the TPR curve of the 1% Rh(O)/MgO indicates two kinds of rhodium compounds, it is reasonable to consider that rhodium was present as Rh_2O_3 and $MgRh_2O_4$, which are responsible for the lower and the higher temperature reduction peaks, respectively. The absence in the XRD patterns of the peaks corresponding to Rh_2O_3 might be a result of its high dispersion over the MgO support. Based on the TPR and XRD results one can conclude that there are much stronger interactions between metal and support for the MgO-supported rhodium catalysts than for the SiO_2-supported ones. As shown in Fig. 2, for the 1% Rh/MgO catalyst, no oscillations of the catalyst temperature occurred during the partial oxidation reaction, while it oscillated as much as 25°C for the 1% Rh/SiO_2 catalyst. This provides additional evidence for the stronger interactions between rhodium and magnesium oxide than between rhodium and silica. Indeed, due to the weak interactions between rhodium and SiO_2, the metallic rhodium formed through the reduction of the oxide by H_2 before the reaction can be reoxidized by O_2 during reaction and the oxide formed can be rereduced again by CH_4, and so on. Because the oxidation and reduction processes are rapid, quasi-adiabatic states can be assumed, and the different enthalpies involved in the two processes lead

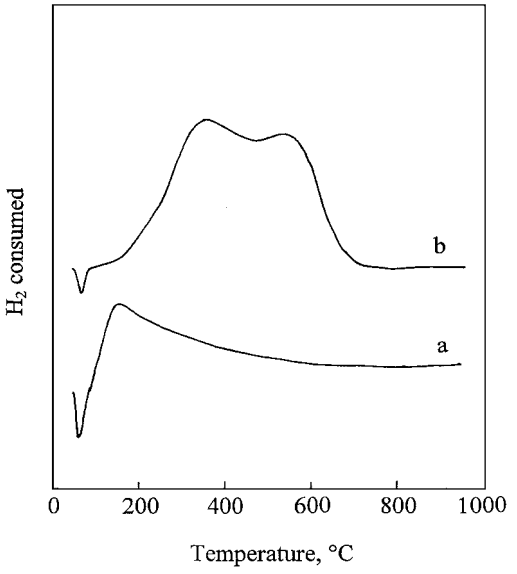

FIG. 6. TPR profiles of 1% Rh(O)/SiO_2 (a) and 1% Rh(O)/MgO (b).

to an oscillatory temperature of the catalyst. In contrast, the much stronger interactions between rhodium and MgO make the reduction to rhodium more difficult and, hence, relatively slow. For this reason, the reduction and oxidation processes become nearer to an isothermal one and no (or little) oscillations of the catalyst temperature will occur.

When CH_4 alone was introduced as pulses over the 1% Rh(O)/MgO catalyst, only total oxidation products, CO_2 and H_2O, were formed during the first three pulses (Fig. 3). Because no oxygen was present in the feed, it is clear that the oxygen contained in Rh_2O_3 and/or $MgRh_2O_4$ was responsible for the CO_2 and H_2O formation. Total oxidation of hydrocarbons is often observed over transition metal oxides even in the absence of gaseous oxygen (36). With the increase in the extent of reduction, the amount of active oxygen (the oxygen of the MgO lattice is inactive) decreased and the number of active Rh sites increased. As a result, the methane conversion decreased (Fig. 3a), but the CO selectivity increased and that of CO_2 decreased (Fig. 3b). It is worth emphasizing that no surface carbon was generated even after the catalyst was almost completely reduced, implying that MgO-supported rhodium catalyst has a low capacity for carbon generation. In contrast, when methane was pulsed over the 1% Rh(O)/SiO_2, not only CO_2 but also surface carbon was formed during the first pulse (Fig. 4b), indicating that methane decomposed to carbon over the rhodium sites formed via the reduction of rhodium oxide by CH_4. With the generation of metallic rhodium, CO and H_2 were detected at the 2nd pulse, implying that rhodium sites are necessary for the formation of CO and H_2. Almost starting with the 2nd pulse, the CH_4 decomposition to carbon dominated the reaction over the 1% Rh(O)/SiO_2 catalyst, indicating that this catalyst has high ability for carbon generation. Of course, the accumulation of surface carbon was responsible for the rapid deactivation of the catalyst which started with the 7th pulse (Fig. 4a). Let us emphasize that in contrast to the SiO_2-supported catalyst, the MgO-supported catalyst was free of carbon deposition under the conditions employed.

Au and Wang compared the reactivities of CH_4/O_2 (2/1) over the oxidized 2.0% Rh(O)/SiO_2 and over the reduced 2% Rh/SiO_2 using the pulse technique and concluded that the oxidized rhodium oxide can be easily reduced by CH_4 even in the presence of O_2 (37). A similar result was obtained in the present work. As shown in Fig. 5, for the first CH_4/O_2 pulse over the 1% Rh(O)/SiO_2 catalyst, the methane conversion was 100% and only total oxidation products, CO_2 and H_2O, were formed. Because the amount of oxygen in the pulse was too small for the total oxidation of CH_4, it is obvious that a part (in fact the largest one) was provided by rhodium oxide. With the generation of rhodium sites, CO started to form at the second pulse, and its selectivity increased sharply reaching rapidly a stable state with increasing number of CH_4/O_2 pulses. This clearly indicates that the metallic rhodium constitutes the active site for the partial oxidation of methane to CO. A notably different behavior was observed over the 1% Rh(O)/MgO. Even though during the first pulse CH_4 was completely converted and CO_2 was the only carbon-containing product formed, unlike the 1% Rh(O)/SiO_2 catalyst, the methane conversion has not remained at the 100% level; on the contrary, it decreased sharply from the 2nd to the 5th pulse, and no CO was formed until the 4th pulse. The pulse experiments also indicated that it is more difficult to reduce the 1% Rh(O)/MgO than the 1% Rh(O)/SiO_2. As suggested by TPR and XRD, two kinds of rhodium compounds, Rh_2O_3 and $MgRh_2O_4$, were present in the 1% Rh(O)/MgO catalyst, with the former more easily reducible than the latter. Both are, however, less reducible than Rh(O)/SiO_2. Because of the difficulty of reduction, the methane conversion decreased rapidly during the following several pulses. With the gradual increase in the extent of reduction, the sites needed for the formation of CO were formed, resulting in an increase in both CO selectivity and methane conversion. However, even at the 15th pulse the methane conversion was still lower than that over 1% Rh(O)/SiO_2 (Fig. 5a), implying that the 1% Rh(O)/MgO catalyst has a much longer induction time. This result is consistent with that obtained in the continuous flow reaction.

The 1% Rh/MgO catalyst provided high methane conversion and selectivities to CO and H_2 with high stability, while the 1% Rh/SiO_2 catalyst rapidly deactivated (Fig. 1).

There are at least two factors that can deactivate the catalyst, namely, the carbon deposition and the sintering of the active metal. By investigating the reactivities of CH_4 over 1% Rh(O)/SiO_2 and over 1% Rh(O)/MgO by the pulse method, we found that a notable amount of surface carbon was formed over the former and none over the latter.

Sintering is especially harmful for supported nickel and noble metal catalysts, because the aggregation of metal crystallites decreases the number of active sites and also accelerates the carbon deposition since larger metal ensembles are beneficial for carbon deposition. For supported nickel catalysts, it has been found that MgO-supported nickel catalysts have stable performances in catalyzing partial oxidation of methane, CO_2 reforming of methane, and the combination of CO_2 reforming and partial oxidation of methane (33, 34, 24). This high stability was attributed to the formation of a solid solution between NiO and MgO. One important implication of the formation of the NiO/MgO solution is that the reduction of NiO occurs with some difficulty, and, as a result, a relatively small amount of Ni is segregated as small particles on the surface of the support. Little sintering occurs because of their strong interactions with the support. In the present paper, the MgO-supported rhodium catalyst was found to have a activity much more stable than that of the SiO_2-supported rhodium catalyst. The strong interactions between rhodium and magnesium oxide (especially

the formation of $MgRh_2O_4$ in the precursor catalyst) are most likely responsible for the high stability. It can be inferred that a relatively uniform dispersion of rhodium oxide on MgO support is generated due to the formation of $MgRh_2O_4$. This compound is reduced with difficulty to at most tiny rhodium crystallites. Some are reoxidized and this redox process is continued. After an induction time, on the order of 10 h for the present conditions, a quasi-steady state for the number of rhodium sites is achieved that is responsible for the conversion of methane. The strong interactions between rhodium and magnesium oxide hinder the aggregation of metallic rhodium and hence its sintering. As a result, the activity of the MgO-supported catalyst can remain constant with the time on stream for a long time (at least 100 h). On the contrary, since no strong interactions between rhodium and SiO_2 exist, rhodium oxide can be easily reduced and the crystallites sinter, leading to the deactivation of the SiO_2-supported rhodium catalysts. In conclusion, the strong interactions between rhodium and magnesium oxide (especially the formation of $MgRh_2O_4$) identified in the present paper are responsible for the highly stable activity of the MgO-supported rhodium catalyst.

5. CONCLUSION

This paper shows that the high stability of the MgO-supported rhodium catalysts is due to the strong interactions between rhodium and magnesium oxide. The identification of $MgRh_2O_4$ (magnesium rhodium oxide) in the precursor catalyst provides direct evidence for the existence of these strong interactions. The TPR and pulse reaction of CH_4/O_2 (2/1) experiments indicate that the reduction of the oxidized MgO-supported rhodium catalysts occurs with greater difficulty than that of the oxidized SiO_2-supported rhodium catalysts. The temperature recordings show that no oscillations of the catalyst temperature occur during the partial oxidation reaction over the 1% Rh/MgO catalyst unlike over the 1% Rh/SiO_2. These results provide additional indirect evidence for the existence of strong interactions between rhodium and magnesium oxide. Because of the strong interactions, the aggregation of the rhodium crystallites is hindered, and thus the sintering of rhodium can be greatly lessened. As a result, the activity of the MgO-supported catalysts can remain constant with the time on stream for a long time.

REFERENCES

1. Hutchings, G. J., Scurell, M. S., and Woodhouse, J. R., *Chem. Soc. Rev.* **18**, 25 (1989).
2. Lunsford, J. H., *Catal. Today* **6**, 235 (1990).
3. Pitchai, R., and Klier, K., *Catal. Rev.—Sci. Eng.* **28**, 13 (1986).
4. Fox, J. M., III, *Catal. Rev. Sci. Eng.* **35**, 169 (1993).
5. Solbakken, A., *in* "Natural Gas Conversion" (A. Holmen, Ed.), p. 447. Elsevier, Amsterdam, 1991.
6. Farina, G. L., and Supp, E., *Hydrocarbon Process.* **71**, 77 (1992).
7. Hickman, D. A., and Schmidt, L. D., *J. Catal.* **138**, 267 (1992).
8. Bhattacharaya, A. K., Breach, J. A., Chand, S., *et al., Appl. Catal. A: General* **80**, L1 (1992).
9. Hickman, D. A., Haupfear, E. A., and Schmidt, L. D., *Catal. Lett.* **17**, 223 (1993).
10. Hickman, D. A., and Schmidt, L. D., *Science* **259**, 343 (1993).
11. Torniainen, P. M., Chu, X., and Schmidt, L. D., *J. Catal.* **146**, 1 (1994).
12. Bharadwaj, S. S., and Schmidt, L. D., *Fuel Process. Technol.* **42**, 109 (1995).
13. Witt, P. M., and Schmidt, L. D., *J. Catal.* **163**, 465 (1996).
14. Nakagawa, K., Ikenaga, N., Suzuki, T., *et al., Appl. Catal. A: General* **169**, 281 (1998).
15. Prettre, M., Eichner, C., and Perrin, M., *Trans. Faraday Soc.* **43**, 335 (1946).
16. Dissanayake, D., Rosynek, M. P., Kharas, K. C. C., and Lunsford, L. H., *J. Catal.* **132**, 117 (1991).
17. Vermeiren, W. J. M., Blomsma, E., and Jacobs, P. A., *Catal. Today* **13**, 427 (1992).
18. Choudhary, V. R., Mamman, A. S., and Sansare, S. D., *Angew. Chem. Int. Ed. Engl.* **31**, 1189 (1992).
19. Choudhary, V. R., Rajput, A. M., and Prabhakar, B., *J. Catal.* **139**, 326 (1993).
20. Chu, Y., Li, S., Lin, J., *et al., Appl. Catal. A: General* **134**, 67 (1996).
21. Choudhary, V. R., Uphade, B. S., and Mamman, A. S., *J. Catal.* **172**, 281 (1997).
22. Miao, Q., Xiong, G., Sheng, S., *et al., Appl. Catal. A: General* **154**, 17 (1997).
23. Lu, Y., Liu, Y., and Shen, S., *J. Catal.* **177**, 386 (1998).
24. Tang, S., Lin, J., and Tan, K. L., *Catal. Lett.* **51**, 169 (1998).
25. Drago, R. S., Jurczyl, K., Kob, N., Bhattacharyya, A., and Masin, *J. Catal.* **51**, 177 (1998).
26. Chen, P., Zhang, H. B., Lin, G. D., and Tsai, K. R., *Appl. Catal. A: General* **166**, 343 (1998).
27. Ashcroft, A. T., Cheetham, A. K., and Foord, J. S., *et al., Nature* **344**, 319 (1990).
28. Jones, R. H., Ashcroft, A. T., Waller, D., *et al., Catal. Lett.* **8**, 169 (1991).
29. Slagtern, A., and Olsbye, U., *Appl. Catal. A: General* **110**, 99 (1994).
30. Choudhary, V. R., Uphade, B. S., and Belhekar, A. A., *J. Catal.* **163**, 312 (1996).
31. Lago, R., Bini, G., Pena, M. A., and Fierro, J. L. G., *J. Catal.* **167**, 198 (1997).
32. Borowiecki, T., *Appl. Catal.* **10**, 273 (1984).
33. Ruckenstein, E., and Hu, Y. H., *Appl. Catal. A: General* **133**, 149 (1995).
34. Ruckenstein, E., and Hu, Y. H., *Ind. Eng. Chem. Res.* **37**, 1744 (1998).
35. Hu, Y. H., and Ruckenstein, E., *Ind. Eng. Chem. Res.* **37**, 2333 (1998).
36. Haber, J., *in* "Surface Properties and Catalysis by Non-Metals" (J. P. Bonnelle, B. Delmon, and E. Derouane, Eds.), p. 1. Reidel, Dordrecht, 1982.
37. Au, C. T., and Wang, H. Y., *J. Catal.* **167**, 337 (1997).